Performance of intra-chip wireless interconnect using on-chip antennas and UWB radios

Sun, Mei; Zhang, Yue Ping; Zheng, Guo Xin; Yin, Wen Yan

2009

Sun, M., Zhang, Y. P., Zheng, G. X., & Yin, W. Y. (2009). Performance of intra-chip wireless interconnect using on-chip antennas and UWB radios. IEEE Transactions On Antennas And Propagation, 57(9), 2756-2762.

https://hdl.handle.net/10356/93567

https://doi.org/10.1109/TAP.2009.2024458

Performance of Intra-Chip Wireless Interconnect Using On-Chip Antennas and UWB Radios

Mei Sun, Yue Ping Zhang, Guo Xin Zheng, and Wen-Yan Yin, *Senior Member, IEEE*

***Abstract*—An intra-chip wireless interconnect system using on-chip antennas and ultrawideband (UWB) radios that operates in 22–29 GHz is studied in this paper. The on-chip antennas are meander monopoles of axial length 1 mm in silicon technology. A unique wireless channel is formed between a pair of on-chip transmit and receive antennas. The channel is characterized up to an interconnect distance of 40 mm. The system performance is evaluated in terms of bit-error-rate (BER) under the assumptions of perfect system synchronization and signal corruption from thermal and switching noises. As expected, the system performance degrades with interconnect distance and data rate. It achieves a better BER on the 5-kΩ.cm Si substrate than that on the 10-Ω.cm Si substrate.**

***Index Terms*—Bit-error-rate (BER), intra-chip wireless interconnect, on-chip antenna, ultrawideband (UWB) radio.**

I. Introduction

SEMICONDUCTOR technologies continuously scale down feature size to improve the speed of operation while enabling much higher degree of integration. However, this scaling implies much greater challenge of wired interconnect because wire width and space are greatly reduced and fundamental material limits are approaching [1]. In order to circumvent this problem, the wireless interconnect using on-chip antennas has been proposed. It uses radio waves rather than metal wires to communicate among cores within a chip (intra-chip) or among chips within a module (inter-chip) [2]–[5].

With the transmission data rate grows linearly with channel bandwidth, the intra-chip wireless interconnect using on-chip antennas and UWB radios appears to have a great advantage to achieve the intra-chip high data transmission for future ultralarger scale integration (ULSI) [6]. Literature survey shows that research on intra-chip wireless interconnect is being undertaken through the following stages.

The first stage is the design and measurement of on-chip antennas. The dipole antennas are usually preferred because they are differential and can adequately reject common-mode noise and interfering signals generated by other circuits on the same silicon substrate as proved by experiments in [6]. However, unavailable differential testing facilities limit the measurement to 26.5 GHz. There is no such limitation for monopoles. Recently a study reported in [7] also reveals that the vertically-excited monopole has better performance than the horizontally-excited dipole in silicon technology. It implies the monopole also has its advantages to be used for intra-chip wireless interconnect.

The second stage is the characterization of the intra-chip radio channel using on-chip antennas. In the frequency domain, the transmission gain is widely used as a channel parameter and measures to improve it are intensively investigated. For example, Kim and O found that the transmission gain of dipoles has higher value on the silicon-on-sapphire (SOS) substrate than those on the bulk and silicon-on-insulator (SOI) substrate [8]. The bulk silicon substrate is lossy due to the low resistivity; while the high resistivity substrate has a lower substrate loss and therefore a higher transmission gain as proved by S. Watanabe *et al.* [9]. It was also found that the interference structures may increase or decrease the transmission gain depending on their layouts [10], [11]. In the time domain, the path loss and delay spread are used as intra-chip radio channel parameters as firstly examined by Zhang *et al.* [12]. Based on the frequency domain study, for an intra-chip radio channel with Si integrated dipoles Kim *et al.* proposed a intuitive plane wave model to explain the propagation mechanisms [13]. Based on both frequency- and time-domain studies, Zhang *et al.* analyzed the different types of propagation waves over the intra-chip channel [12]. Nevertheless, propagation mechanisms of the intra-chip wireless channel still needs further studying and particularly modeling.

The third stage is the performance evaluation of the intra-chip wireless interconnect using on-chip antennas and UWB radios. Using the discrete UWB pulse forming networks, sampling oscilloscope, and bit error rate tester (BERT), K. Kimoto *et al.* presented the experimental data transmission characteristics of the intra-chip wireless interconnect using 6 mm long integrated linear dipole antennas at 13.5 Gbps and found that the BER performance was 1.6×10^{-2} [14]. However, no theoretical analysis was presented.

The fourth stage is the circuit implementation of the intra-chip wireless interconnect, which is probably the most challenging stage. With a single-chip CMOS UWB transmitter for intra-chip wireless interconnect presented in [15], it is believed

Manuscript received January 01, 2008; revised February 10, 2009. First published June 05, 2009; current version published September 02, 2009. This work was supported in part by the Natural Science Foundation of China under Grant 90607011 and in part by the Research Grant Council of Hong Kong under project HKU7165/05E .

M. Sun is with the Institute for Infocomm Research, Singapore 138623, Singapore (e-mail: msun@i2r.a-star.edu.sg).

Y. P. Zhang is with the School of Electrical and Electronic Engineering, Nanyang Technological University, Singapore 639798, Singapore (e-mail: eypzhang@ntu.edu.sg).

G. X. Zheng is with the School of Communication and Information Engineering, Shanghai University, Shanghai 200072, China.

W.-Y. Yin is with the Center for Optical and EM Research, Zhejiang University, Hangzhou 3100, China.

Color versions of one or more of the figures in this paper are available online at http://ieeexplore.ieee.org.

Digital Object Identifier 10.1109/TAP.2009.2024458

that the implementation of the real intra-chip wireless interconnect using on-chip antennas and UWB radios in a single chip is becoming more and more feasible with high-frequency silicon technologies and ever-increasing chip size for intra-chip communication.

In this paper, we study an intra-chip wireless interconnect using on-chip meander monopole antennas and UWB radios that operates in 22–29 GHz in silicon technology. Section II presents the on-chip meander antenna performance. Section III characterizes the intra-chip wireless channel. Section IV evaluates the intra-chip wireless interconnect performance. Finally, Section V summarizes the conclusions. From antenna to system, we go through the three stages of studies and provide a methodology to analyze the intra-chip wireless interconnect both in channel prorogation mechanism and theoretical performance evaluation aspects.

II. On-Chip Meander Antenna

The on-chip meander monopole is used as transmit antenna (TA) and receive antenna (RA) for intra-chip wireless interconnect with d varied at 2.5, 5, 10, 20, 30, and 40 mm as shown in Fig. 1(a). With its wire folded back and forth the antenna resonance is found in a much more compact structure than can otherwise be obtained. Fig. 1(a) shows its top view photograph. The axial length of the antenna is 1 mm. The test ground-signal-ground (GSG) pads are squares of 80 μm by 80 μm. The width of the line elements is 10 μm. The antenna was fabricated using the NTU 1.2-μm CMOS process on silicon wafers of high resistivity 5-kΩ.cm and low resistivity 10-Ω.cm, respectively. Fig. 1(b) shows its cross sectional view. It is seen that an oxide layer of thickness 2 μm was grown on the silicon substrate of thickness 633 μm to increase isolation and an aluminum layer of thickness 2 μm was used to form the antenna [16].

Fig. 2(a) shows the simulated and measured return losses as a function of frequency for the fabricated on-chip meander antennas. The simulation was made using the Zeland IE3D software package. The measurement was conducted on wafer with Cascade Microtech coplanar Probes and an HP8510XF network analyzer. It is seen that the locations of the resonance dips agree well for both high and low resistivity cases. They are at 23 and 18 GHz for the 5-kΩ.cm Si and 10-Ω.cm Si substrates, respectively. The feature size of our meander antenna is about 2.5 mm. Based on the exact simulations from the IE3D, it is found that the guided wavelengths at 23 GHz in the 5-kΩ.cm Si substrate and at 18 GHz in the 10-Ω.cm Si substrate of Fig. 1(b) are both about 5 mm. This indicates that the origin of these resonant frequencies comes from the half-wavelength resonance. Also note that there are differences between the simulated and measured return loss values. This is because in the measurement the probe station was connected to the on-chip meander antenna. However, the probe effect was not included in the IE3D model as no detailed information on the probe was available. The probe ground enhanced the on-chip ground pads, changed the impedance matching conditions, and caused the differences. Further note from Fig. 2(a) that for the 5-kΩ.cm Si substrate the measured 6-dB impedance bandwidth is 22–32 GHz and for the 10-Ω.cm Si substrate the measured 8-dB impedance bandwidth

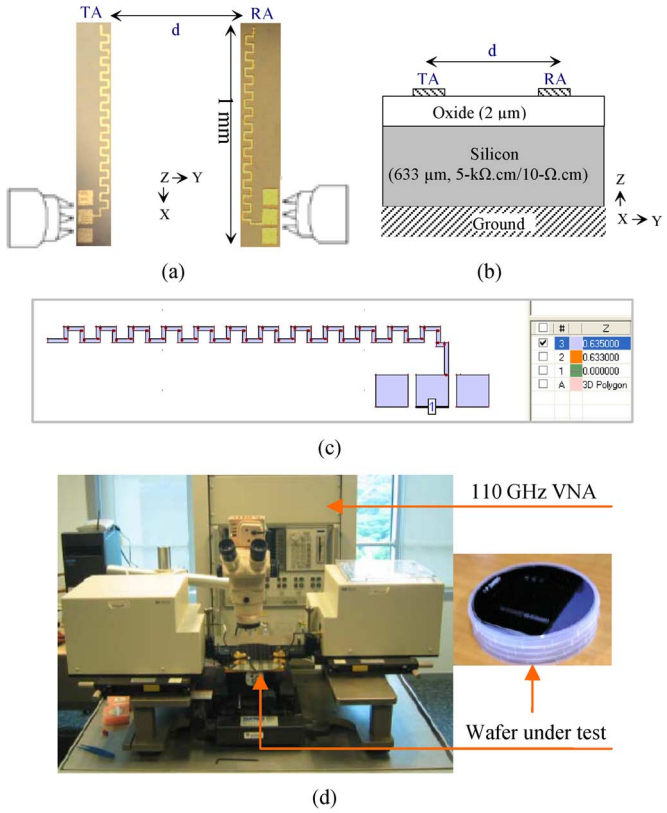

Fig. 1. On-chip meander antenna: (a) top view photograph with probe touching illustration, (b) cross-sectional view of the test vehicle, (c) IE3D model, and (d) photograph of the wafer under test.

is 15–31 GHz. The return loss results are both larger than 6 dB from 22–29 GHz, indicating an acceptable matching to a 50-Ω source.

Fig. 2(b) and (c) shows the simulated far-field radiation patterns in the azimuth and elevation planes at 25 GHz, taking RA with denoted coordinate system of Fig. 1(a) as an example. It is noted that in the elevation plane, the radiation patterns, both co- and cross-polarizations can only be obtained for the upper hemisphere because the electromagnetic model assumes infinite extension of the ground plane. As expected, for both high and low resistivity cases, the maximum co-polarization radiation occurs in the 0° direction. In addition, the cross-polarization is found weaker than the co-polarization radiation, especially for high resistivity case. In the azimuth plane, for both high and low resistivity cases the maximum co-polarization radiation occurs in the $\varphi = 195°$ direction and the cross-polarization radiations are found to be more than 30 dB weaker than the co-polarization radiations.

Fig. 2(d) shows the simulated antenna gain values as a function of frequency. The IE3D calculates a gain value as 4π times the ratio of an antenna's radiation intensity in a given direction to the total power accepted by the antenna. As expected, the higher gain is achieved for high resistivity case. The gain values obtained here will be used to model the transmission coefficient between the TA and RA in the Part B of Section III. In addition, it is noted that the simulated radiation efficiency from 22 to 29 GHz is 60 $\sim$ 77% for the 5-kΩ.cm Si substrate and 9 $\sim$ 14% for the 10-Ω.cm Si substrate, respectively.

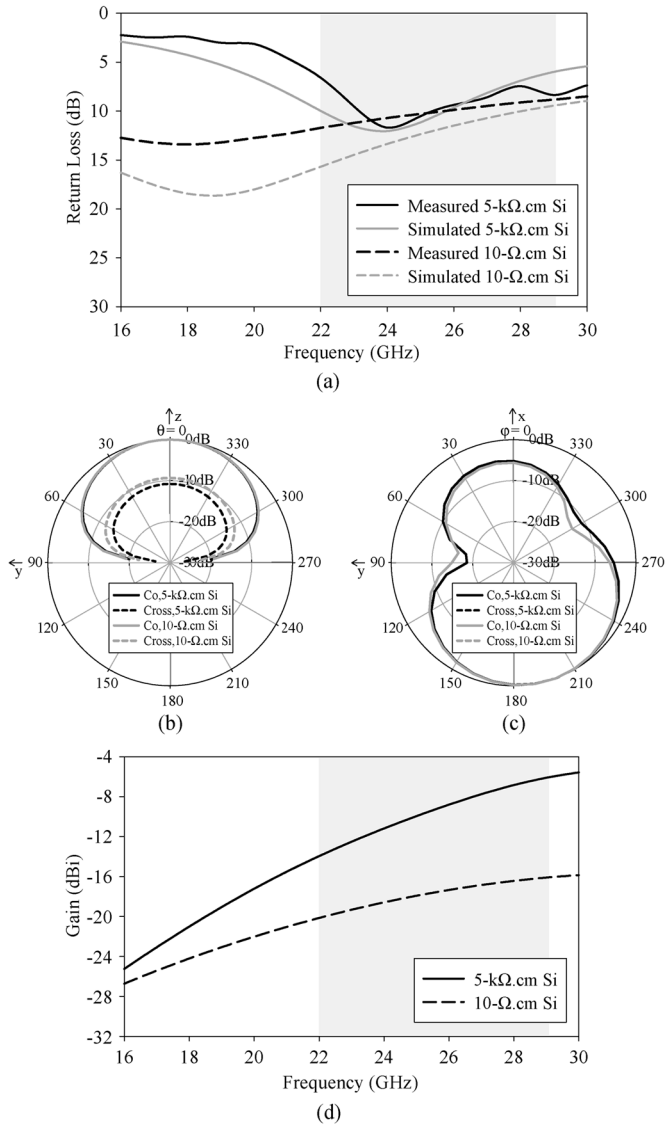

Fig. 2. Performance of the on-chip meander antenna: (a) return loss, (b) azimuth plane (YZ-plane, $\varphi = 90°$) radiation patterns at 25 GHz, and (c) elevation plane (XY-plane, $\theta = 85°$) radiation patterns at 25 GHz, and (d) gains.

III. Characterization of Intra-Chip Wireless Channel

A unique intra-chip wireless channel is formed between the TA and RA. The TA and RA pairs, each the mirror image of the other, were layout in a test vehicle with the T-R separation distance d varied at 2.5, 5, 10, 20, 30, and 40 mm. The cross sectional view of the test vehicle is the same as in Fig. 1(b). The test vehicle was fabricated on both 10-$\Omega.\mathrm{cm}$ and 5-k$\Omega.\mathrm{cm}$ 6-in p-type silicon wafers and measured to characterize the intra-chip wireless channel as shown in Fig. 1(d) [16]. The sensitivity limit of the measurement system is about -70 dBm. It is found that the received signal for the 10-$\Omega.\mathrm{cm}$ Si substrate case can not be distinguished from the noise when the separation distance is up to 20 mm. While for the 5-k$\Omega.\mathrm{cm}$ Si substrate case the effective transmission still can be supported up to a distance of 40 mm. The time domain analysis in the Part *C* of this section will give the explanation on it.

A. Frequency-Domain Measurement

A transfer function H is defined in the frequency domain for the intra-chip wireless channel as the ratio of the signal applied to the TA to the signal received by the RA. Fig. 3 shows the measured H on the 10-$\Omega.\mathrm{cm}$ and 5-k$\Omega.\mathrm{cm}$ Si substrates. It is seen that both amplitude and phase of the transfer function H fluctuate with frequency. As expected the amplitudes of H are higher for the 5-k$\Omega.\mathrm{cm}$ Si substrate than those for the 10-$\Omega.\mathrm{cm}$ Si substrate at the same interconnect distance. The loss of the intra-chip wireless channel depends on the chip substrate resistivity. The higher the resistivity is, the lower the loss is [9].

The propagation rather than the reactive coupling plays an important role in the intra-chip wireless transmission. This mechanism is supported by Fig. 3(c) and (d) that shows the relationship between the phase delay and frequency. To our knowledge, if reactive coupling played the key role, the phase delay would either keep constant over frequency or follows the sum of a few $arctan$ functions of frequency. In addition, the speed of electromagnetic wave is extracted by the phase variation $\Delta\varphi(H)$ and the T-R distance variation Δd as follows [16]:

$$v = \frac{2\pi f}{\frac{\Delta\varphi(H)}{\Delta d}}. \tag{1}$$

The calculated speed v is $\sim 0.95 \times 10^8$ m/s $\approx 0.3\,c$, where c is the speed in free space. The effective relative permittivity is further estimated as $\varepsilon_{\text{eff}} = (c/v)^2 \approx 10$. It is very close to the silicon relative permittivity of $\varepsilon = 11.9$ signifying that the dominant medium supporting the wave propagation is the silicon substrate. This agrees well with the conclusion in [17]. For the antenna formed on a substrate with $\varepsilon = 11.9$ it is expected $\varepsilon^{3/2}$ times more power radiated into the substrate than into free space [18].

B. Frequency-Domain Modeling

The IE3D is used for frequency-domain modeling in the range where the interested separation distance is comparable to the wavelength. However, with increased distance between elements compared with wavelength the high-oscillating part of the subintegral in method of MOM matrix elements makes standard integration procedures inapplicable [19], which makes IE3D inaccurate. A statistical ray-tracing model is then developed for this frequency range. Fig. 4 shows a simplified ray tracing model in accordance with the Fig. 1(b). The rays which travel through the top oxide layer are neglected because the oxide thickness is negligibly small compared to a wavelength. The bottom ground plane or metal chuck of a probe station makes the rays reflect off it. The nth path traveled by the mth ray with the transmit angle of θ_{i} picked by the RA has the gain as follows:

$$G_{mn}(f,d)=\begin{cases} T_1 e^{-\lambda_2 l_2} T_2 e^{-\lambda_3 l_3} R_3 e^{-\lambda_3 l_3} \\ \quad \times T_2' e^{-\lambda_2 l_2} T_1' \left(R_2' R_3 e^{-2\lambda_3 l_3}\right)^n & 0<\theta_i<90° \\ e^{-\lambda_1 d} & \theta_i = 90° \\ 0 & \text{others} \end{cases} \tag{2}$$

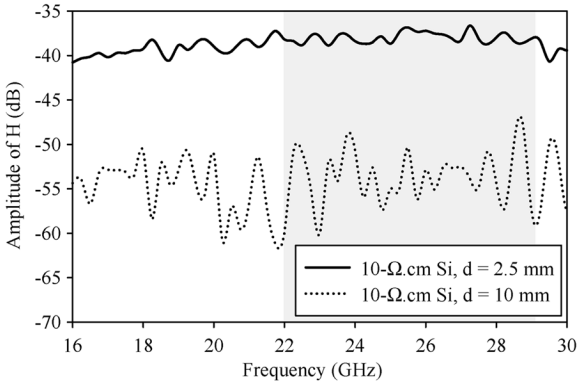

(a)

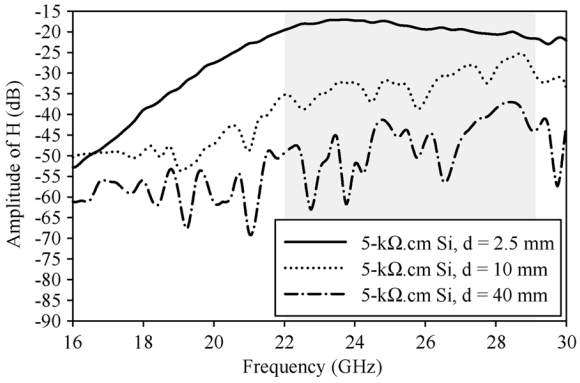

(b)

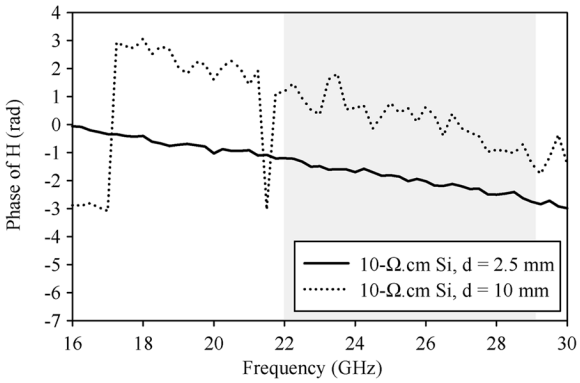

(c)

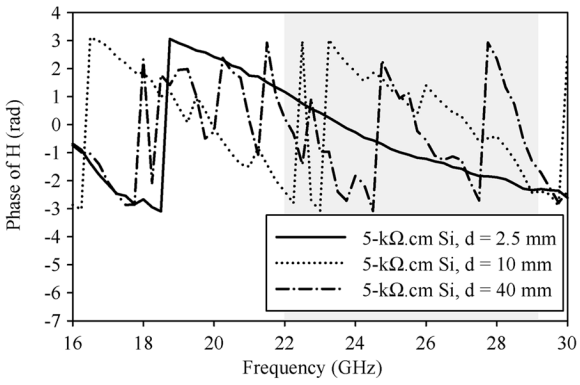

(d)

Fig. 3. Measured channel transfer function H: (a) amplitude for the 10-$\Omega.\mathrm{cm}$ Si substrate, (b) amplitude for the 5-k$\Omega.\mathrm{cm}$ Si substrate, (c) phase for the 10-$\Omega.\mathrm{cm}$ Si substrate, and (d) phase for the 5-k$\Omega.\mathrm{cm}$ Si substrate.

where R_i, T_i, R_i', and T_i' represent the Fresnel's reflection and transmission coefficients at the ith planar interface, used for different ray direction as shown in Fig. 4. They are calculated using two polarizations cases [20]. l_i is the path length traveled by the wave through the ith layer. d is the T-R separation distance. λ_i is the complex propagation constant in the ith layer. The transfer function H between TA and RA then can be calculated by (3) using the statistical method for N_test rays, where G_ta and G_ra are the simulated gains for TA and RA, respectively, as shown in Fig. 2(d). The *limit* is the observation limit as shown in Fig. 4. As seen the simulated transfer function H is d, f dependant

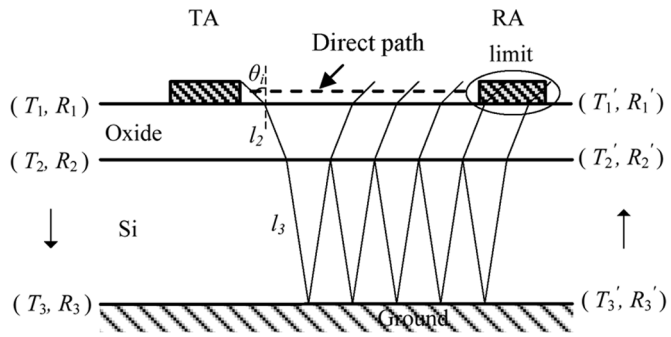

Fig. 4. The simplified ray tracing model.

$$H(f,d)=\sqrt{\frac{1}{N_\mathrm{test}}\sum_{m}^{\leq \mathrm{limit}}\left(\left|G_{ta}(f)G_{ra}(f)\sum_{n=1}^{N_\mathrm{m}}G_{mn}(f,d)\right|\right)^2}. \tag{3}$$

The modeling results of the amplitude of H are presented in Fig. 5(a) and (b) for both low and high resistivity Si cases. It is found that the modeling results agree with 10 measurements data averaged values. This confirms the mechanism behind this modeling as presented in [16]. That is in the frequency range where the separation distance is relatively comparable with wavelength the IE3D EM simulator can model this case well. However in the frequency range where the separation distance is relatively larger than wavelength the statistical ray-tracing model is more accurate because the multiple propagation paths (rays) are supported by the intra-chip wireless channel. This causes the fluctuations in the amplitudes of the transfer function as clearly shown in Fig. 3(a) for 10 mm and (b) for 40 mm separation distance. The intra-chip wireless channel can thus be regarded as a frequency-selective channel.

C. Time-Domain Analysis

The channel impulse response is firstly obtained by the Inverse discrete Fourier transform (IDFT) of the measured transfer function H. The wide measurement frequency ensures a fine time domain resolution. Based on it, the received power delay profile, path loss and delay spread are obtained for analysis.

The received power delay profile peak for the antenna pair on 10-$\Omega.\mathrm{cm}$ Si substrate has been found to be heavily attenuated by more than two orders of magnitude as compared to that for antennas on 5-k$\Omega.\mathrm{cm}$ Si substrate. In addition, with a noise floor set to 10 dB above average noise [12] the received power delay profile is entirely buried in noise when the TA-RA separation increased to a limit which is found as 20 mm for 10-$\Omega.\mathrm{cm}$

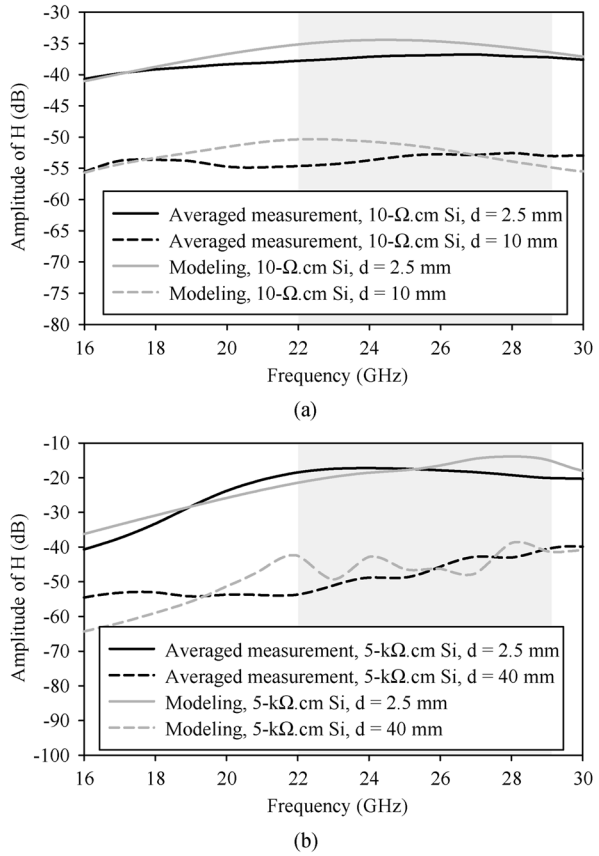

Fig. 5. Modeling results compared with averaged measurement results for the amplitude of H: (a) 10-$\Omega.\mathrm{cm}$ Si substrate and (b) 5-k$\Omega.\mathrm{cm}$ Si substrate.

Si substrate and 40 mm for 5-k$\Omega.\mathrm{cm}$ Si substrate, respectively. For brevity no plots are presented here. Because the transmitting power and receiving sensitivity of our measurement set up are limited, we can only choose the useful data within these distance limits to analyze and further reveal the channel propagation mechanism.

Table I lists the path loss PL that represents the power attenuation due to the intra-chip wireless channel for both resistivity cases. It is found from Fig. 6 that scatter PL values are fitted well by the equation shown in the figure with quite small σ, where γ, d_0, PL_0 are the path loss factor, reference distance and intercepted PL at d_0 respectively. X_σ is a zero-mean Gaussian-distributed random variable in dB with standard deviation σ. It is noted that γ is significantly lower than the free-space value of 2, implying the signal is not carried through the space wave. The spherical behavior of space wave with distance further enhances this conclusion. Leaky wave is not considered due to that it decreases exponentially over the intra-chip channel thus contributes negligibly to the received signal. Guided wave is realized via the reflection within the wafer and attenuated greatly due to the lossy wafer, especially for larger T-R distance. Surface wave occurs near the interface between the air and wafer. Thus it is believed that surface wave constitutes the dominant contribution as T-R distance increases because of its cylindrical characteristics. With the ratio of substrate thickness and the free-space wavelength t/λ_0 is >0.045 at 22–29 GHz the

TABLE I
PATH LOSS VERSUS DISTANCE

	PL (dB)	
Distance (mm)	5-kΩ.cm Si	10-Ω.cm Si
2.5	26.10	43.21
5	31.24	48.53
10	36.45	52.66
20	38.50	-
40	42.05	-

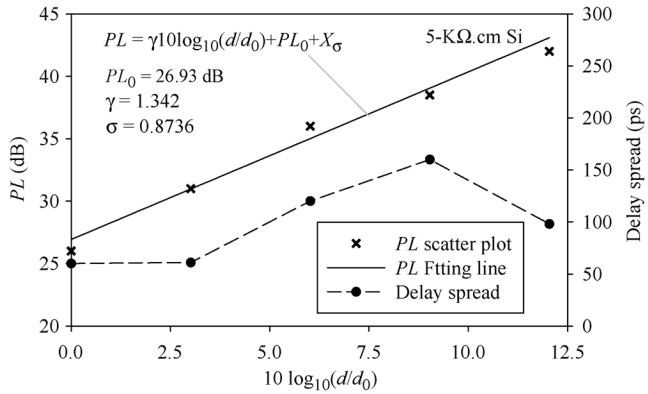

Fig. 6. Path loss and delay spread versus log distance.

more energy is expected to be carried by surface wave than by space wave as analyzed in [21]. This conclusion is further enhanced by the observation of the first arrival signal peak, which excludes the possibilities of its transmission through space wave and reflected wave [12]. As a result, it can be summarized that space wave contributes negligibly to the received signal and surface wave is the dominant path of received signal. Integrated antennas for intra-chip communications should be designed to launch effectively the surface wave rather than space wave.

Fig. 6 also shows the delay spread over the log T-R distance. As seen it is generally increases with the distance, signifying that the received signal energy spreads over a longer time span with increased distance [12].

IV. PERFORMANCE OF INTRA-CHIP WIRELESS INTERCONNECT

An intra-chip wireless interconnect system is simulated using the on-chip meander antennas and UWB radios in silicon technology. No experimental verification is made. It operates over a 7-GHz bandwidth from 22–29 GHz. This higher UWB band is preferable because it has higher transmission gain and is less contaminated by the switching noise coupling from the on-chip digital circuitry. The pulse position modulation scheme is adopted in the UWB radio. The BER performance of the intra-chip wireless interconnect system is evaluated according to the approach described in [22] with the following parameters: the receiver gain and noise figure are 20 and 15 dB, respectively; the switch noise is 10 dB lower than the thermal noise; and the implementation loss is -4 dB. The targeted highest data rate is 3.33 Gbps as limited by the designed PPM signal frame width [22]. As expected, the BER performance degrades with interconnect distance and data rate. It achieves a better BER on

the 5-$k\Omega.cm$ Si substrate than that on the 10-$\Omega.cm$ Si substrate. For example, the interconnect on the 5-$k\Omega.cm$ substrate can support a data rate of 3.33 Gbps with a $BER < 10^{-20}$ up to a distance of 40 mm with the average transmitted power of 0 dBm; while the interconnect on the 10-$\Omega.cm$ substrate can support the same data rate with a $BER \approx 10^{-20}$ up to a distance of 10 mm with the same transmitted power.

V. Conclusion

The on-chip meander monopole antennas of axial length 1 mm were fabricated in silicon technology. They were measured and simulated in terms of return loss, radiation patterns and gains. The acceptable matching at 22–29 GHz was obtained.

A unique wireless channel is formed between a pair of on-chip transmit and receive antennas. It was experimentally characterized up to an interconnect distance of 40 mm and its mechanism was analyzed in both frequency and time domains. Based on the analysis in frequency domain it is concluded that the intra-chip wireless channel shows the frequency-selective characteristic. Based on the analysis in time domain it is concluded that propagation of radio waves over intra-chip channels is mainly realized with surface wave rather than space wave. These important characteristics provide some insights to the intra-chip wireless channel mechanism thus provide the guidance for intra-chip wireless system design.

The intra-chip wireless interconnect system using the on-chip meander antennas and UWB radios that operate in 22–29 GHz was finally evaluated in terms of BER under the assumptions of perfect system synchronization and signal corruption from thermal and switching noises. As expected, the BER performance degrades with interconnect distance and data rate. It achieves a better BER on the 5-$k\Omega.cm$ Si substrate than that on the 10-$\Omega.cm$ Si substrate.

References

[1] J. A. Davis *et al.*, "Interconnect limits on Gigascale Integration (GSI) in the 21st century," *Proc. IEEE*, vol. 89, no. 3, pp. 305–324, March 2001.

[2] K. K. O *et al.*, "Inter and intra-chip wireless clock signal distribution using microwaves: A status of an initial feasibility study," in *Proc. Government Microw. Circuit Applicat. Conf.*, Mar. 1999, pp. 306–309.

[3] B. A. Floyd, C. M. Hung, and K. O. Kenneth, "Intra-chip wireless interconnect for clock distribution implemented with integrated antennas, receivers, and transmitters," *IEEE J. Solid State Circuits*, vol. 37, no. 5, pp. 534–552, 2002.

[4] S. Watanabe, K. Kimoto, and T. Kikkawa, "Transient characteristics of integrated dipole antennas on silicon for ultra wideband wireless interconnects," in *Proc. IEEE Antennas and Propag. Society Int. Symp.*, Jun. 2004, vol. 3, pp. 2277–2280.

[5] Y. P. Zhang, "Wireless chip area network: A new paradigm for antennas, RF(MM)ICs, and communications," presented at the Proc. Asia-Pacific Microw. Conf., India, 2004.

[6] M. Nitta and T. Kikkawa, "Interference of digital noise with integrated dipole antenna for inter-chip signal transmission in ULSI," in *IEEE Antennas Propag. Society Int. Symp.*, Jul. 2005, vol. 3B, pp. 264–267.

[7] A. B. M. H. Rashid *et al.*, "Efficient design of integrated antennas on Si for on-chip wireless interconnects in multi-layer metal process," *Jpn. J. Appl. Phys.*, vol. 44, pp. 2756–2760, 2005.

[8] K. Kim and K. K. O, "Characteristics of integrated dipole Antennas on bulk, SOI and SOS substrates for wireless communications," in *IEEE Proc. IITC*, San Francisco, CA, 1998, pp. 21–23.

[9] A. B. M. H. Rashid, S. Watanabe, and T. Kikkawa, "Characteristics of integrated antenna on Si for on-chip wireless interconnect," *Jpn. J. Appl. Phys.*, vol. 42, pp. 2204–2209, 2003.

[10] S. Watanabe, A. B. M. H. Rashid, and T. Kikkawa, "Effect of high resistivity Si substrate on antenna transmission gain for on-chip wireless interconnects," *Jpn. J. Appl. Phys.*, vol. 43, pp. 2297–2301, 2004.

[11] X. L. Guo, R. Li, and K. K. O, "Design guidelines for reducing the impact of metal interference structures on the performance on-chip antennas," in *Proc. IEEE Antennas Propag. Society Int. Symp.*, 2003, vol. 1, pp. 606–609.

[12] Y. P. Zhang, Z. M. Chen, and M. Sun, "Propagation mechanisms of radio waves over intra-chip channels with integrated antennas: Frequency-domain measurements and time-domain analysis," *IEEE Trans. Antennas Propag.*, vol. 55, no. 10, pp. 2900–2906, 2007.

[13] K. Kim *et al.*, "A plane wave model approach to understanding propagation in an intra-chip communication system," in *2001 IEEE Antennas Propag. Society Int. Symp.*, 2001, vol. 2, pp. 166–169.

[14] K. Kimoto and T. Kikkawa, "Data transmission characteristics of integrated linear dipole antennas for UWB communication in Si ULSI," in *IEEE Antennas Propag. Society Int. Symp.*, 2005, vol. 1B, pp. 678–681.

[15] P. K. Saha, N. Sasaki, and T. Kikkawa, "A CMOS UWB transmitter for intra/inter-chip wireless communication," in *Proc. IEEE 8th Int. Symp. on Spread Spectrum Tech. Applicat.*, 2004, pp. 962–966.

[16] M. Sun, Y. P. Zhang, and G. X. Zheng, "Modeling and measurement of the on-chip meander antenna pairs," presented at the Asia-Pacific Microw. Conf., China, 2005.

[17] K. Kim, Y. Hyun, and K. K. O, "On-chip wireless interconnection with integrated antennas," in *Int. Electron Devices Meeting*, 2000, pp. 485–488.

[18] D. B. Rutledge and D. P. Kasilingam, *Integrated and Millimeter Waves*. Boston, MA: Academic Press, 1983.

[19] R. Zentner, Z. Sipus, and J. Bartolic, "Theoretical and experimental study of mutual coupling between microstrip stacked patch antennas," presented at the IEEE Antennas Propag. Society Int. Symp., 2003.

[20] C. A. Balanis, *Advanced Engineering Electromagnetics*. New York: Wiley, 1938.

[21] D. M. Pozar, "Considerations for millimeter wave printed antennas," *IEEE Trans. Antennas Propag.*, vol. AP-31, no. 5, pp. 740–747, Sep. 1983.

[22] M. Sun and Y. P. Zhang, "Performance of inter-chip RF-interconnect using CPW, capacitive coupler and UWB transceiver," *IEEE Trans. Microw. Theory Tech.*, vol. 53, no. 9, pp. 2650–2655, 2005.

Mei Sun received the B.E. and M.E. degrees from the Hunan University and Beijing Institute of Technology, China, in 2000 and 2003, respectively and the Ph.D. degree from Nanyang Technological University (NTU), Singapore, in 2007, all in electronic engineering.

From 2006 to 208, she worked at NTU. She is now a Research Fellow with the Institute for Infocomm Research, Singapore. Her research interests include intra- and inter-chip RF wireless communication system simulation and implementation, as well as millimeterwave and terahertz antenna design.

Dr. Sun was a recipient of the Best Paper Prize from the Third IEEE International Workshop on Antenna Technology, 21–23rd March 2007, Cambridge, U.K.

Yue Ping Zhang received the B.E. and M.E. degrees from Taiyuan Polytechnic Institute and Shanxi Mining Institute of Taiyuan University of Technology, Shanxi, China, in 1982 and 1987, respectively, and the Ph.D. degree from the Chinese University of Hong Kong, Hong Kong, in 1995, all in electronic engineering.

From 1982 to 1984, he worked at Shanxi Electronic Industry Bureau, from 1990 to 1992, the University of Liverpool, Liverpool, U. K., and from 1996 to 1997, City University of Hong Kong. From 1987 to 1990, he taught at Shanxi Mining Institute and from 1997 to 1998, the University of Hong Kong. He was promoted to a Full Professor at Taiyuan University of Technology in 1996. He is now an Associate Professor and the Deputy Supervisor of Integrated Circuits and Systems Laboratories with the School of Electrical and Electronic Engineering, Nanyang Technological University, Singapore. He has broad interests in radio science and technology and published widely across seven IEEE societies. He has delivered scores of

invited papers/keynote address at international scientific conferences. He has organized/chaired dozens of technical sessions of international symposia.

Dr. Zhang received the Sino-British Technical Collaboration Award in 1990 for his contribution to the advancement of subsurface radio science and technology. He received the Best Paper Award from the Second International Symposium on Communication Systems, Networks and Digital Signal Processing, 18–20th July 2000, Bournemouth, UK and the Best Paper Prize from the Third IEEE International Workshop on Antenna Technology, 21–23rd March 2007, Cambridge, UK. He was awarded a William Mong Visiting Fellowship from the University of Hong Kong in 2005. He is listed in *Marquis Who's Who, Who's Who in Science and Engineering, Cambridge IBC 2000 Outstanding Scientists of the 21st Century*. He serves on the Editorial Board of the *International Journal of RF and Microwave Computer-Aided Engineering* and a Guest Editor of the *Journal* for the special issue *RF and Microwave Subsystem Modules for Wireless Communications*. He also serves as an Associate Editor of the *International Journal of Microwave Science and Technology*. Furthermore, he serves on the Editorial Boards of IEEE TRANSACTIONS ON MICROWAVE THEORY AND TECHNIQUES and IEEE MICROWAVE AND WIRELESS COMPONENTS LETTERS.

Guo Xin Zheng received the B.E. and M.E. degrees from Taiyuan Polytechnic Institute and Shanxi Mining Institute of Taiyuan University of Technology, Shanxi, China, in 1982 and 1987, respectively, both in electronic engineering.

He taught at Shanxi Mining Institute from August 1987 to June 1996. He was a Visiting Research Fellow at the Chinese University of Hong Kong from May to August 1994. He was a Full Professor at Taiyuan University of Technology from 1998 to August 2000. Since September 2000, he has been Deputy Dean and Professor of the School of Communication and Information Engineering, Shanghai University, China. From June to August 2004, he was a Visiting Professor of the School of Electrical and Electronic Engineering, Nanyang Technological University, Singapore. His research interests are in the area of radio communications and automatic control.

Dr. Zheng received the 1996 Outstanding Yong Scientist Award from Shanxi Provincial Government.

Wen-Yan Yin (M'99–SM'08) received the M.Sc. degree in electromagnetic field and microwave technique from Xidian University (XU), Shaanxi, China, in 1989 and the Ph.D. degree in electrical engineering from Xi'an Jiaotong University (XJU), Xi'an, China, in 1994.

From 1993 to 1996, he worked in the Department of Electronic Engineering, Northwestern Polytechnic University (NPU). From 1996 to 1998, he was a Research Fellow with the Department of Electrical Engineering, Duisburg University, granted by the Alexander von Humblodt-Stiftung of Germany. Since December 1998, he has been a Research Fellow with the Monolithic Microwave Integrated Circuit (MMIC) Modeling and Packing Laboratory, Department of Electrical Engineering, National University of Singapore (NUS), Singapore. In March 2002, he joined Temasek Laboratories, NUS, as a Research Scientist and the Project Leader of high-power microwave and ultrawideband electromagnetic compatibility (EMC)/electromagnetic interference (EMI). In April 2005, he joined the School of Electronic Information and Electrical Engineering, Shanghai Jiao Tong University (SJTU), Shanghai, China, as a Chair Professor in Electromagnetic Fields and Microwave Techniques (until 2007). He is now the Director of the Center for Microwave and RF Technologies, SJTU. Since 2009, he has been Qie Shi Chair Professor at Zhejiang University (ZJU), working in the Center for Optics and Electromagnetic Research, Department of Optical and Electrical Information. His main research interests are EMC, EMI, and EM protection; on-chip passive and active MM(RF)IC devices and circuits modeling, design, and packaging; ultrawideband interconnects and signal integrity, and nonoelectronics. As a leading author, he has published more than 150 international journal articles including 15 book chapters. One chapter, "Complex Media," is included in the *Encyclopedia of RF and Microwave Engineering* (Wiley, 2005). His main research interests are in electromagnetic characteristics of complex media and their applications in engineering, EMC, EMI, and electromagnetic (EM) protection, on-chip passive and active MM (RF) IC device testing, modeling, and packaging, ultra-wideband interconnects and signal integrity, and Nanoelectronics.

Prof. Yin is the Technical Chair of Electrical Design of Advanced Packaging and Systems (EDAPS'06), technically sponsored by IEEE CPMT Subcommittee; and he won the Best Paper Award of the 2008 APEMC and 19th International Zurich Symposium on EMC in Singapore. He is a Reviewer of international journals including six IEEE TRANSACTIONS, *Radio Science, Inst. Elect. Eng. Proceedings-H, Microwave, Antennas, and Propagation*, .